



Published in final edited form as:

*Nano Lett.* 2011 March 9; 11(3): 1076–1081. doi:10.1021/nl103951e.

## Nanoengineered Surfaces Enhance Drug Loading and Adhesion

Kathleen E. Fischer<sup>1,2</sup>, Aishwarya Jayagopal<sup>1</sup>, Ganesh Nagaraj<sup>1</sup>, R. Hugh Daniels<sup>3</sup>, Esther M. Li<sup>3</sup>, Matthew T. Silvestrini<sup>1</sup>, and Tejal A. Desai<sup>1,2,\*</sup>

Kathleen E. Fischer: kayte@berkeley.edu; Aishwarya Jayagopal: aishjay07@gmail.com; Ganesh Nagaraj: gnagaraj87@gmail.com; R. Hugh Daniels: HDaniels@nanosysinc.com; Esther M. Li: ELi@nanosysinc.com; Matthew T. Silvestrini: silve200@umn.edu; Tejal A. Desai: Tejal.Desai@ucsf.edu

<sup>1</sup> Department of Bioengineering and Therapeutic Sciences, UCSF; San Francisco, CA 94158

<sup>2</sup> UCSF/UCB Joint Graduate Group in Bioengineering; San Francisco, CA 94158

<sup>3</sup> Nanosys, Inc.; Palo Alto, CA 94304

### Abstract

To circumvent the barriers encountered by macromolecules at the gastrointestinal mucosa, sufficient therapeutic must be delivered in close proximity to cells<sup>1</sup>. Previously, we have shown that silicon nanowires penetrate the mucous layer and adhere directly to cells under high shear<sup>2</sup>. In this work, we characterize potential reservoirs and load macromolecules into space created between nanowires. We show significant increases in loading capacity due to nanowires while retaining adhesion of loaded particles under high shear.

### Keywords

Nanowires; adhesion; drug delivery; hierarchical nanostructures

---

Mucosal tissues, such as those lining the oral cavity and gastrointestinal tract, have great potential for delivery of therapeutic macromolecules, but drug absorption is often thwarted by chemical and physical barriers. The epithelia is covered in a 1–50  $\mu\text{m}$  motile mucus gel layer with pores of roughly 100 nm<sup>3–5</sup>. Like chyme, which clears the entire small intestine within 150 to 240 minutes<sup>6, 7</sup>, the mucus layer turns over every 50–170 minutes<sup>8</sup>. As a result of the viscosity and motility of the mucus, therapeutic macromolecules take longer to diffuse to cells, increasing their susceptibility to degradation and removal<sup>1</sup>.

Adhesion and encapsulation technologies have been developed to combat the harsh gastrointestinal environment. Increased residence time in the upper small intestine and adhesion in close proximity or directly to cells increases the local concentration gradient at the epithelial layer, promoting transport<sup>9–11</sup>. Encapsulation in polymers, microparticles, or nanoparticles can protect therapeutics from degradation, ensuring that they remain active until they are released near the tissue.

Numerous adhesives have been developed with the intent of increasing microparticle gastrointestinal residence time. However, most chemical adhesives function through mucoadhesion, primarily attaching to the mucus layer on top of the tissue, and thus being

---

\*Additional contact information for Tejal A. Desai: Tejal.Desai@ucsf.edu, phone – 415–514–4503, fax – 415–476–2414.

Supporting Information Available: Further descriptions of the methods used in this paper, as well as theoretical surface area and geometry calculations and discussion, elution curves, and a consideration of loading capacity and therapeutic efficacy are available in the Supporting Information section. This material is available free of charge via the Internet at <http://pubs.acs.org>.

removed within a few hours<sup>12</sup>. Recent advances in nanotechnology have produced drug-encapsulating nanoparticles of varying materials and geometries. Although these nanoparticles can cross the mucus barrier and can be endocytosed relatively quickly<sup>13</sup>, because of their small size, nanoparticles lose a considerable fraction of loading volume to the encapsulation material<sup>14, 15</sup>, and may lead to potentially toxic accumulations in the liver, kidneys, and spleen<sup>16, 17</sup>. Microparticles can be fabricated with hollow reservoirs or engineered pores using photolithography, etching, or anodization<sup>9, 18</sup>. Although these technologies significantly improve loading capacity compared to nanoparticles, the additional fabrication complexity considerably increases the overall cost of the devices, and the larger size reduces diffusion through the mucus layer.

We have shown that integrating the diffusive properties at the nanoscale, in the form of a conformal silicon nanowire coating, with size and loading capacity of microparticles can result in direct microparticle-cell adhesion through structure alone, creating a significantly more robust adhesive<sup>2, 19</sup>. Here we show that a nanoengineered microparticle (NEMP) system offers a simple alternative to complex fabrication of hollow reservoirs and pores comprised of a reservoir between the nanowires at their base where drug may be loaded, thus displaying adhesion and loading in a single platform.

In this work, solid NEMPs and controlled pore glass particles (collectively termed “devices”) were characterized for adsorptive surface area, then loaded with model molecules and tested for elution properties. Using a surface tension loading approach, therapeutics were loaded into a reservoir formed by the base of the nanowires, leaving the exterior portion of the nanowires free to adhere to cells. Furthermore, variations in nanowire length and loading solution concentration were evaluated to optimize the loading capacity of nanowire coatings. Lastly, loaded devices were introduced to cells and subjected to shear flow of a model mucous layer to determine the effect of loading on adhesion.

Nanowire length, and thus surface area, has been shown to affect adhesion to cells<sup>2</sup> and may affect device loading volume. Increased surface area due to the nanowires may improve loading capacity by providing a surface for protein to adsorb; alternately, increased nanowire length can enlarge the space available to create a loading reservoir at the base of the nanowires. Using Krypton gas to measure adsorptive surface area, we found that the nanowires increase surface area roughly in proportion to their length (see Supporting Information); ie: 1.4  $\mu\text{m}$  long nanowires increase surface area roughly 1.5-fold over uncoated controls and 12.1  $\mu\text{m}$  long nanowires increase surface area roughly 12.8-fold. Nonetheless, relying on a 10 to 20-fold increase in surface area for protein adsorption due to nanowires is not sufficient to carry therapeutic levels of drug.

Thus, devices were loaded with trypan blue, bovine serum albumin (BSA), insulin, and immunoglobulin G (IgG) using an evaporation technique allowing surface tension and capillary action to draw drug into the pores between nanowires and/or onto the surface of the devices (Figure 1a). During loading, capillary forces pull molecules into the base of the nanowires similar to how drugs were loaded into nanotubes or pores<sup>10, 20–22</sup>. A washing step was necessary in order to remove debris and drug not incorporated into the devices. Devices were imaged prior to elution experiments to determine the distribution of drug within the nanowires or on the surface (Figure 1.b and c). At this stage, the nanowire-coated devices demonstrated minimal matting of the nanowires enmeshed in crystals.

Loaded CPG particles were then placed in solution and elution was measured up to a week (data is only presented up to 48 hours because of the degradation time for model proteins). The model molecules can be classified into different groups based on their elution characteristics. Larger molecules, including insulin (6 kDa), BSA (66 kDa), and IgG (150

kDa), tended to have a longer term release as molecules captured at the base of the nanowires or in the pores elute (Figure 2.a and b show typical curves for IgG at 2.5 hr and 48 hr, other curves are available in the Supporting Information). IgG and insulin showed nearly linear elution profiles to 24 hours ( $r^2$  values of both were 0.99) and eluted 15.0 mg and 18.9 mg of protein per ml devices in that time, respectively, comparing favorably to the volume of drug necessary to make a therapeutic impact (see Supporting Information). Smaller molecules like trypan blue had a burst release, with nearly all molecules eluted by 30 minutes.

Despite its larger molecular weight, IgG has one of the highest elution volumes. Since IgG requires salts to solubilize significantly<sup>23</sup>, more of the other model proteins may be rinsed off of the devices during the rinse step, resulting in a comparatively lower elution. A similar effect may explain the high elution volumes of insulin, which is poorly soluble at neutral pH. Overall, the amount of drug eluted from nanowire-coated particles was greater than uncoated particles for each molecule (significant at  $\alpha=0.01$  for all molecules). This finding suggests that the nanowires add an additional reservoir for drug, presumably at their base.

To test this hypothesis, microspheres without pores were loaded with BSA (Figure 3). Microspheres with longer nanowires held significantly more drug than those with short or no nanowires. This suggests that longer nanowires create a larger reservoir at their base. Although the CPG particles could load some BSA even without nanowires (Figure 3.b), the nanowires significantly increase the loading capacity of the CPG. Elution curves for the nanowire-coated devices without pores (3.a and 3.c) show an initial burst release within 40–60 minutes that is most likely coming from the protein that has adsorbed onto the outer portions of the nanowires allowing them to be more quickly released into solution. The rest of the material is “caked” into the nanowire matrix, which takes longer to reconstitute and longer to elute. Thus, the lack of pores in the microspheres did not decrease loading in nanowire-coated devices, confirming that the nanowire are responsible for an additional drug reservoir.

Nanowire-coated microspheres were loaded at various concentrations of BSA to determine a maximum effective loading capacity (Figure 4). Although the nanowires are visible and mainly uncoated at 1 and 10 mg/ml, at 50 and 100 mg/ml loading solutions the wires become more matted, indicating saturation. When loaded devices are incubated in PBS, the spheres loaded with higher concentrations (50 and 100 mg/ml) elute roughly the same amount of BSA, significantly more than that eluted from the 10 mg/ml spheres (Figure 3c). Thus, increasing loading solution concentration increases the amount of drug loaded into the nanowire reservoir, though it saturates around 50 mg/ml.

Because loading drug molecules into the nanowire reservoir could mask nanowires from cells, thereby reducing adhesion, the loaded devices were tested for adhesion strength under shear. Devices were introduced to cells in a mucous layer model (2% Type II porcine gastric mucin), then subjected to increasing flow rates.

Loaded, nanowire-coated, CPG particles adhered significantly better than loaded, uncoated CPG particles (Figure 5.a). Nearly 60% of nanowire-coated CPG were retained at 167 dynes/cm<sup>2</sup>. The CPG particles are non-spherical, so the orientation of the longer sides to the surface will reduce the particle flow profile<sup>10, 24</sup>; a low shear helps particles situate optimally, increasing the surface area of devices in contact with cells, as is observed up to 16.7 dynes/cm<sup>2</sup> in this case.

The levels of loading also affected adhesion (Figure 5.b), reducing adhesion significantly at physiological shears (up to 15 dynes/cm<sup>2</sup>). A general trend confirmed that particles that were loaded in more concentrated solutions, leading to more matted and masked nanowires,

did not adhere as well as those with less drug loading. Thus, there is an optimal level of loading that allows for enough volume of therapeutic to be included, but does not impair adhesion significantly. Perhaps a loading concentration of 50 mg/ml in this case might make sense, since in figure 3c, we can see that the elution from a 50 and 100 mg/ml concentration elutes similarly, and in figure 5b, we can see that 50 mg/ml loading concentration does not impair adhesion as much as 100 mg/ml loading concentration. Ultimately, devices with longer nanowires could be fabricated, allowing significantly more drug to be loaded without losing adhesion.

Long silicon nanowires have been shown to increase adhesion in numerous cell types and under various harsh conditions<sup>2, 19</sup>. This work shows that these nanowires can also have another function – as a loading reservoir for therapeutic molecules of different sizes. Compared to controlled pore glass, the reservoir created at the base of the nanowires holds significantly more volume of drug molecules. Longer nanowires, which create a more voluminous nanowire shell on the exterior of the devices, offer a greater loading capacity. Although there is a tradeoff between adhesive strength and loading volume, devices with suitable volumes of drug can still retain significant adhesive strength (as in the case of the CPG particles and the 50 mg/ml loaded spheres). Furthermore, because nanowires may be grown up to 40  $\mu\text{m}$ , a much larger loading capacity may be realizable without impacting adhesion.

In addition to composing a structure-mediated adhesive, nanowires also create a sizable reservoir at their base, able to carry and elute 15–20 mg of protein per ml of device. In this work, we chose to focus on a proof of concept, device optimization, and the effects of loading on nanowire adhesion. Because silicon nanowires may be chemically modified to carry targeting molecules on the wire or specifically on the tip<sup>25</sup>, a simple nanowire coating provides at least three significant functionalities to a drug delivery device: targeting, adhesion, and a loading reservoir. Integrating the nanoengineered loading reservoir into a multifunctional, hierarchical device simplifies processing and fabrication, and improves the scalability of this type of system.

Furthermore, nanowire coatings may be useful for delivering drugs to numerous mucosal surfaces, such as nasal, buccal, oral, ocular, and vaginal tissue<sup>19</sup>. Nanowires adhere strongly to numerous tissue types and are robust under many conditions. Because of their strength, adhesion, and loading capacity, nanoengineered, structure-mediated functional platforms may prove useful for adhesives, drug-eluting coatings for medical implants, or tissue regeneration surfaces as well as drug delivery.

## Supplementary Material

Refer to Web version on PubMed Central for supplementary material.

## Acknowledgments

Microscopy was done at the UCSF Nikon Imaging Center with the help of Kurt Thorn. KF was supported by an NSF Graduate Research Fellowship. This research was conducted with funding from NIH grant EB01166401, a Rogers Foundation Grant and from a University of California Discovery Grant, with partnership from Nanosys, Inc.

## References

1. Khanvilkar K, Donovan MD, Flanagan DR. Drug transfer through mucus. *AdV Drug DeliVery Rev* 2001;48:173.

2. Fischer KE, Aleman BJ, Tao SL, Daniels RH, Li EM, Bunger MD, Nagaraj G, Singh P, Zettl A, Desai TA. Biomimetic Nanowire Coatings for Next Generation Adhesive Drug Delivery Systems. *Nano Lett* 2009;9(2):716–720. [PubMed: 19199759]
3. Ponchel G, Irache J. Specific and non-specific bioadhesive particulate systems for oral delivery to the gastrointestinal tract. *Adv Drug Del Rev* 1998;34:191–219.
4. Smart JD. The basics and underlying mechanisms of mucoadhesion. *Adv Drug Del Rev* 2005;57:1556–1568.
5. Cone RA. Barrier properties of mucus. *Adv Drug Del Rev* 2009;61(2):75–85.
6. Degen LP, Phillips SF. Variability of gastrointestinal transit in healthy women and men. *Gut* 1996; (39):299–305. [PubMed: 8977347]
7. Camilleri M, Colemont LJ, Phillips SF, Brown ML, Thomforde GM, Chapman N, Zinsmeister AR. Human gastric emptying and colonic filling of solids characterized by a new method. *AJP - Gastrointestinal and Liver Physiology* 1989;257(2):G284–290.
8. Lehr CM. An estimate of turnover time of intestinal mucus gel layer in the rat in situ loop. *Int J Pharm* 1991;70:235.
9. Foraker AB, Walczak RJ, Cohen MH, Boiarski TA, Grove CF, Swaan PW. Microfabricated porous silicon particles enhance paracellular delivery of insulin across intestinal Caco-2 cell monolayers. *Pharm Res* 2003;20(1):110–116. [PubMed: 12608544]
10. Tao SL, Desai TA. Gastrointestinal patch systems for oral drug delivery. *Drug Discov Today* 2005;10(13):909–915. [PubMed: 15993810]
11. Eaimtrakarn S, Rama Prasad YV, Puthli SP, Yoshikawa Y, Shibata N, Takada K. Possibility of a patch system as a new oral delivery system. *Int J Pharm* 2003;250(1):111–117. [PubMed: 12480277]
12. Bies C, Lehr CM, Woodley JF. Lectin-mediated drug targeting: history and applications. *Adv Drug Delivery Rev* 2004;56:425.
13. Lai SK, Wang Y-Y, Hanes J. Mucus-penetrating nanoparticles for drug and gene delivery to mucosal tissues. *Adv Drug Del Rev* 2009;61(2):158–171.
14. Kumar V, Prud'homme RK. Thermodynamic limits on drug loading in nanoparticle cores. *J Pharm Sci* 2008;97(11):4904–4914. [PubMed: 18300278]
15. Freitas S, Merkle HP, Gander B. Microencapsulation by solvent extraction/evaporation: reviewing the state of the art of microsphere preparation process technology. *J Controlled Release* 2005;102(2):313–332.
16. Teeguarden JG, Hinderliter PM, Orr G, Thrall BD, Pounds JG. Particokinetics In Vitro: Dosimetry Considerations for In Vitro Nanoparticle Toxicity Assessments. *Toxicol Sci* 2007;95(2):300–312. [PubMed: 17098817]
17. Sanvicens N, Marco MP. Multifunctional nanoparticles - properties and prospects for their use in human medicine. *Trends Biotechnol* 2008;26(8):425–433. [PubMed: 18514941]
18. Tasciotti E, Liu X, Bhavane R, Plant K, Leonard AD, Price BK, Cheng MMC, Decuzzi P, Tour JM, Robertson F, Ferrari M. Mesoporous silicon particles as a multistage delivery system for imaging and therapeutic applications. *Nature Nanotechnology* 2008;3:151–157.
19. Fischer KE, Nagaraj G, Daniels RH, Li E, Cowles VE, Miller JL, Bunger MD, Desai TA. Hierarchical Nanoengineered Surfaces for Enhanced Cytoadhesion and Drug Delivery. Submitted to *Nature Materials*. 2010
20. Anglin EJ, Cheng L, Freeman WR, Sailor MJ. Porous silicon in drug delivery devices and materials. *Adv Drug Del Rev* 2008;60(11):1266–1277.
21. Salonen J, Laitinen L, Kaukonen AM, Tuura J, Björkqvist M, Heikkilä T, Vähä-Heikkilä K, Hirvonen J, Lehto VP. Mesoporous silicon microparticles for oral drug delivery: Loading and release of five model drugs. *J Controlled Release* 2005;108 (2–3):362–374.
22. Salonen J, Kaukonen AM, Hirvonen J, Lehto VP. Mesoporous silicon in drug delivery applications. *J Pharm Sci* 2008;97(2):632–653. [PubMed: 17546667]
23. Gagnon, P. Use of Hydrophobic Interaction Chromatography with a Non-Salt Buffer System for Improving Process Economics in Purification of Monoclonal Antibodies. *Waterside Conference on Monoclonal and Recombinant Antibodies*; Florida USA: Miami; 2000.

24. Tao, SL. Off-wafer fabrication of asymmetric, polymeric gastrointestinal micropatch systems: Characterization of caco-2 monolayer binding and compatibility. Boston University; Boston: 2006.
25. Desai, T.; Fischer, KE.; Nagaraj, G.; Kim, Y.; Jayagopal, A.; Daniels, H.; Li, E. Nano-structure based bioadhesive drug delivery. NanoEngineering for Medicine and Biology; Houston, TX, Houston, TX: 2010.

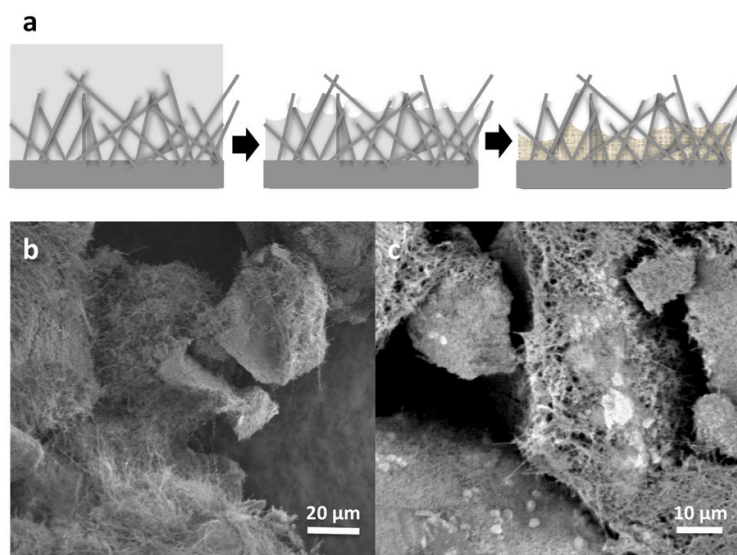


**Figure 1.** Drug loading. A) schematic of nanowire drug reservoir. As solution evaporates, drug molecules are pulled into the base of the nanowires by capillary action, then crystallize there, leaving the exterior nanowires exposed. Stock (b) and loaded (c) controlled pore glass devices. Devices were loaded with bovine serum albumin.



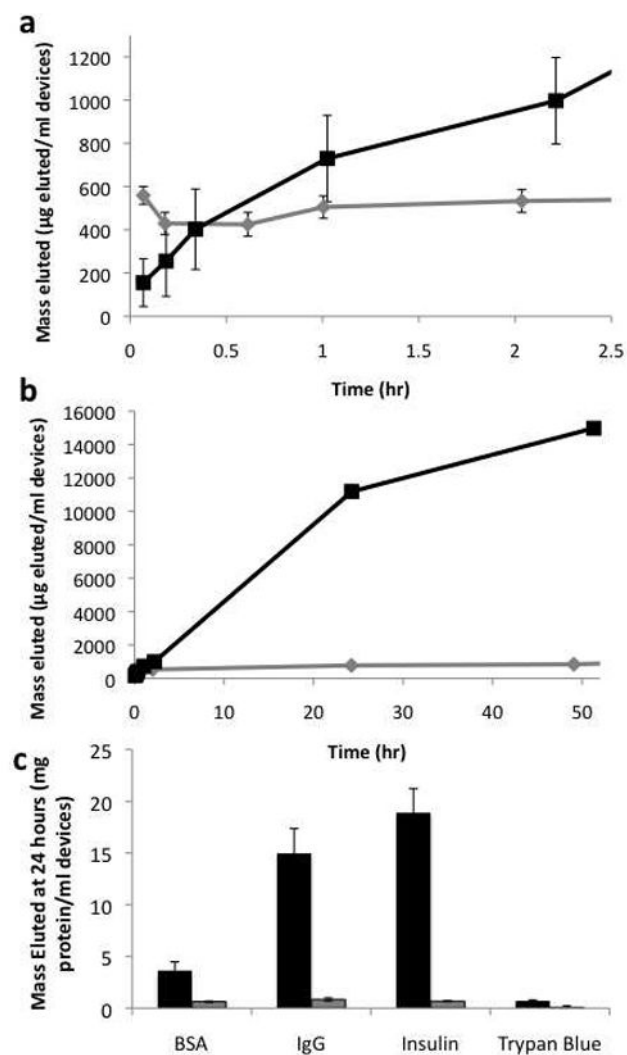


**Figure 2.** Elution from controlled pore glass devices. A) and B) Elution of IgG from nanowire-coated devices (black) and uncoated devices (gray) for 2.5 hours (A) and 48 hours (B). C) Total elution at 48 hours. Nanowire-coated devices – black, uncoated devices – gray. Error bars on all plots are standard error of the mean.



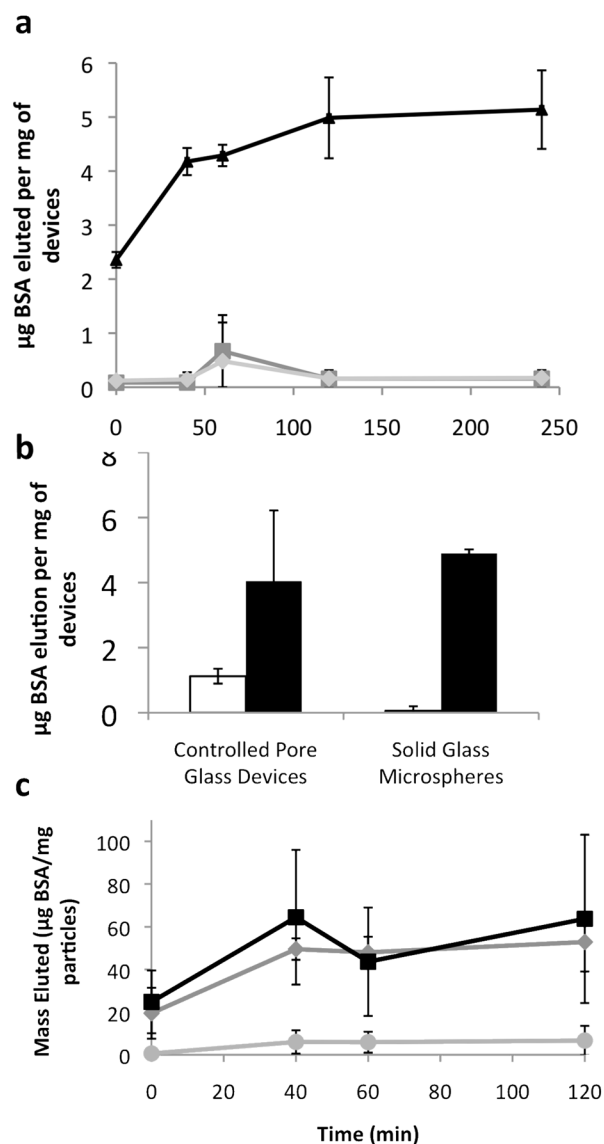


**Figure 3.** Elution from nanowire-coated spheres. A) Spheres with different nanowire lengths (no nanowires - square, short nanowires - diamond, and long nanowires - triangle). Error bars are standard deviation. B) Elution of bovine serum albumin (BSA) for a given weight of devices at 2 hr. Despite having pores, the controlled pore glass without nanowires (white) did not elute as much BSA as the devices with nanowires (black), indicating that the majority of the loading is happening in the nanowires. Error bars indicated standard error of the mean. C) Spheres with various loading concentrations (10 mg/ml – circle, 50 mg/ml – diamond, 100 mg/ml – square). Error bars are standard deviation.

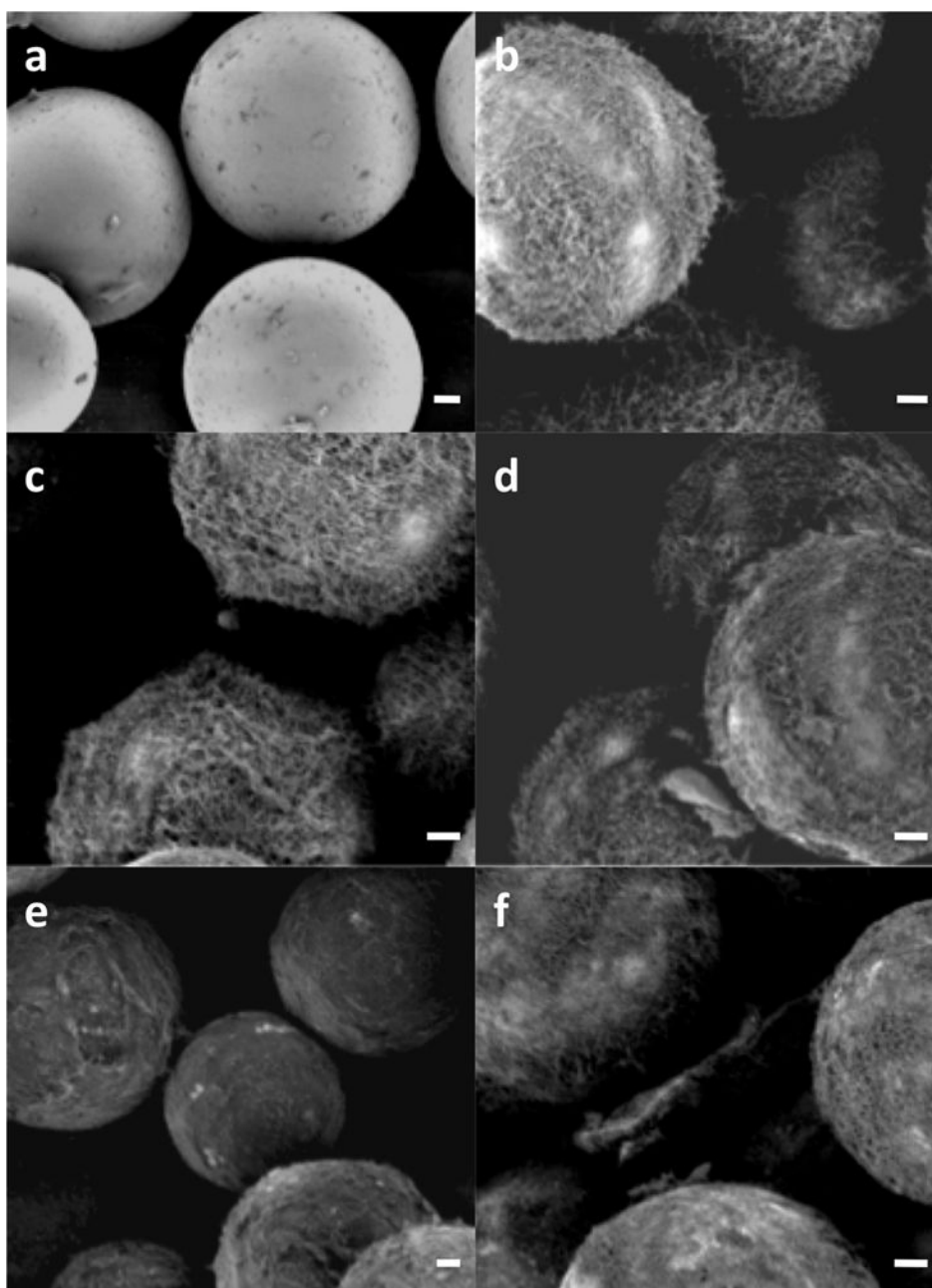


**Figure 4.** Loaded and unloaded microspheres. a) Unloaded control spheres. B) unloaded nanowire-coated spheres. C–f) 1, 10, 50, and 100 mg/ml loaded (respectively). Scale bar is 5  $\mu\text{m}$  in all images.

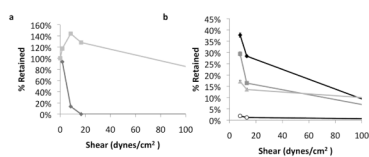


**Figure 5.** Adhesion of loaded particles. A) Adhesion for nanowire-coated controlled pore glass devices loaded with albumin (nanowire-coated – gray square, uncoated control – black diamond). Error bars are standard deviation. B) Adhesion for nanowire-coated spheres loaded with varying concentrations of albumin (unloaded – black diamond, 10 mg/ml – dark gray square, 50 mg/ml – light gray triangle, 100 mg/ml – white circle). Error bars are 95% confidence intervals as calculated for a Kaplan Meier Survival Curve.